Characterization of integrated photonic devices with minimum phase technique

Halir, R.; Molina-Fernández, Í.; Wangüemert-Pérez, J. G.; Ortega-Moñux, A.; De-Oliva-Rubio, J.; Cheben, P.

Publisher's version / Version de l'éditeur:
https://doi.org/10.1364/OE.17.008349
Optics Express, 17, 10, pp. 8349-8361, 2009

Characterization of integrated photonic devices with minimum phase technique

R. Halir,[1,*] Í. Molina-Fernández,[1] J.G. Wangüemert-Pérez,[1] A. Ortega-Moñux,[1] J. de-Oliva-Rubio,[1] P. Cheben[2]

[1] *Departamento Ingeniería de Comunicaciones, ETSI Telecomunicación, Universidad de Málaga, 29071 Málaga, Spain*

[2] *Institute for Microstructural Sciences, National Research Council of Canada, Ottawa, ON, K1A 0R6, Canada*

robert.halir@ic.uma.es

Abstract: Spurious reflections can preclude the accurate experimental characterization of integrated optical devices. This is particularly important for facet reflections in high refractive index platforms such as Indium Phosphide (InP) or Silicon-on-Insulator (SOI) when no anti-reflective (AR) coating is used. In this paper we present a novel method to recover the original device characteristics from the measured power transmission in the presence of such reflections. Our approach uses minimum phase techniques to reconstruct time domain information which is filtered to remove the reflection artifacts. A criterion to assess if a certain device exhibits the minimum phase characteristics required to apply the technique is given. Simulated and experimental results for multi-mode interference couplers (MMICs) in SOI without AR coating validate the technique.

OCIS codes: (230.3120) Integrated optics devices; (120.5700) Reflection; (220.4840) Testing

References and links

1. R. G. Walker, "Simple and accurate loss measurement technique for semiconductor optical waveguides," Electron. Lett. **21**, 581–583 (1985).
2. W. J. Tomlinson, A. Shahar, and R. J. Deri, "Use and misuse of end-facet reflections in the characterization of optical waveguide directional couplers," Appl. Opt. **30**, 2961–2969 (1991).
3. C. Vázquez, P. Baquero, and F. Hernández-Gil, "Fabry-Perot method for the characterization of integrated optical directional couplers," Appl. Opt. **34**, 6874–6886 (1995).
4. B. J. Soller, D. K. Gifford, M. S.Wolfe, and M. E. Froggatt, "High resolution optical frequency domain reflectometry for characterization of components and assemblies," Opt. Express **13**, 666–674 (2005).
5. Y. Gottesman, E. Rao, and D. Rabus, "New methodology to evaluate the performance of ring resonators using optical low-coherence reflectometry," J. Lightwave Technol. **22**, 1566–1572 (2004).
6. M. Muriel and A. Carballar, "Phase reconstruction from reflectivity in uniform fiber Bragg gratings," Opt. Express **22**, 93–95 (1997).
7. A. Carballar and M. Muriel, "Phase reconstruction from reflectivity in fiber Bragg gratings," J. Lightwave Technol. **15**, 1314–1322 (1997).
8. A. Ozcan, M. Digonnet, and G. Kino, "Characterization of Fiber Bragg Gratings Using Spectral Interferometry Based on Minimum-Phase Functions," J. Lightwave Technol. **24**, 1739 (2006).
9. A. Ozcan, M. Digonnet, and G. Kino, "Minimum-phase-function-based processing in frequency-domain optical coherence tomography systems," J. Opt. Soc. Am. A **23**, 1669–1677 (2006).
10. A. Ozcan, M. Digonnet, and G. Kino, "Iterative processing of second-order optical nonlinearity depth profiles," Opt. Express **12**, 3367–3376 (2004).
11. J. Skaar and H. Engan, "Phase reconstruction from reflectivity in fiber Bragg gratings," Opt. Lett. **24**, 136–138 (1999).

#106382 - $15.00 USD Received 14 Jan 2009; revised 3 Mar 2009; accepted 4 Mar 2009; published 1 May 2009

12. L. Poladian, "Group-delay reconstruction for fiber Bragg gratings in reflection and transmission," Opt. Lett. **22**, 1571–1573 (1997).
13. J. McDaniel and C. Clarke, "Interpretation and identification of minimum phase reflection coefficients," J. Acoust. Soc. Am. **110**, 3003–3010 (2001).
14. A. V. Oppenheim and R. W. Schafer, *Discrete-Time Signal Processing* (Prentice-Hall International, 1989).
15. K. Rochford and S. Dyer, "Reconstruction of minimum-phase group delay from fibre Bragg grating transmittance/reflectance measurements," Electron. Lett. **35**, 838–839 (1999).
16. J. Fienup, "Reconstruction of an object from the modulus of its Fourier transform," Opt. Lett. **3**, 27–29 (1978).
17. S. J. Mason, "Feedback Theory — Further Properties of Singal Flow Graphs," Proc. IRE **44**, 920–926 (1956).
18. J. Victor, "Temporal impulse responses from flicker sensitivities: causality, linearity, and amplitude data do not determine phase," J. Opt. Soc. Am. A **6**, 1302–3 (1989).
19. A. V. Oppenheim and R. W. Schafer, *Digital Signal Processing* (Prentice Hall, 1975).
20. R. V. Churchill and J. W. Brown, *Variable Compleja y Aplicaciones* (McGraw-Hill, 1990).
21. A. Ozcan, M. Digonnet, and G. Kino, "Quasi-phase-matched grating characterization using minimum-phase functions," Opt. Commun. **269**, 199–205 (2007).
22. R. Halir, I. Molina-Fernández, A. Ortega-Moñux, J. G. Wangüemert-Pérez, D.-X. Xu, P. Cheben, and S. Janz, "A Design Procedure for High Performance, Rib Waveguide based Multimode Interference Couplers in Silicon-on-Insulator," J. Lightwave Technol. **26**, 2928–2936 (2008).

1. Introduction

Characterization of integrated optical devices in research environments is often performed with a tunable laser source (TLS) as input and a detector at the device output which records the transmitted optical power as a function of wavelength. When a high refractive index platform, such as InP or SOI, is used, power reflections at the chip facets can be very strong ($\sim 30\%$ of the power is reflected at SOI facets). In a waveguide this results in the well known Fabry-Perot fringes, which can be used to calculate propagation losses [1]. However, for devices with several inputs and outputs more complicated interference patterns arise, because of the multiple sources of reflection. As an example, Fig. 1 shows actual measurement data of a SOI 2×3 multimode interference coupler (MMIC), in a prototyping setup that will be described in section 4.3. The amplitude of the interference fringes is of 5 dB, thus completely obscuring the actual device response which is only expected to vary approximately 1 dB in the $1520-1580$ nm band. Hence it is often necessary to cover the chip facets with an anti-reflective coating prior to measurement. Nevertheless, the ability to measure propagation losses of reference waveguides on the chip, using the Fabry-Perot technique, is then lost. Furthermore, from cost point of view, it might be preferable to coat only those devices which are known to function correctly. This is why several methods have been proposed to characterize devices without anti-reflective coating [2, 3]. These are however limited to specific coupler configurations and depend on the value of the facet reflection coefficient.

In this paper we present a technique that combines the concepts of Minimum Phase and Temporal Filtering (MPTF), to completely remove the interference fringes arising from spurious reflections. We show that using minimum phase techniques it is possible to compute meaningful time domain information, which is then filtered to eliminate the reflection artifacts and recover the desired device characteristics. The temporal data can be computed directly from the swept laser measurement of the chip. It is conceptually analogous to that obtained by Optical Frequency Domain Reflectometry (OFDR) [4], and could also be used for other time domain characterization techniques, such as [5]. Minimum phase techniques have been applied to the characterization of Fiber Bragg Gratings [6, 7, 8], optical tomography [9] and the characterization of nonlinear films [10] among others. The key issue of these techniques is to ensure that the system which is being analyzed actually exhibits minimum phase characteristics [11, 12, 13]; if these are not fulfilled the accuracy of the technique is often affected negatively. Here, we present a comprehensive theoretical analysis of the MPTF technique, and derive a minimum phase condition for optical systems, which is in agreement with previously published experi-

#106382 - $15.00 USD Received 14 Jan 2009; revised 3 Mar 2009; accepted 4 Mar 2009; published 1 May 2009

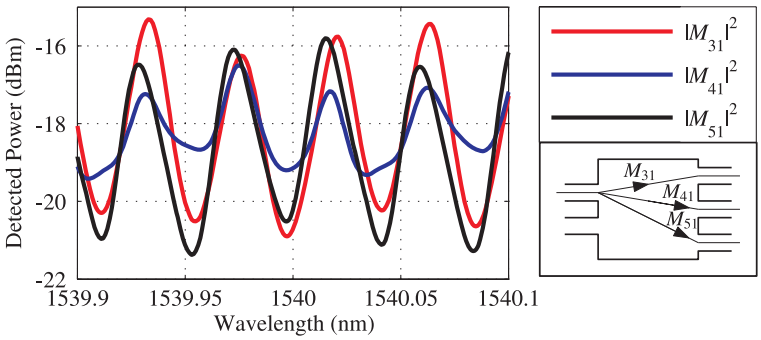

Fig. 1. Measured transmittance of a 2×3 MMIC in SOI without AR coating.

mental results, and can be used to assess the applicability of the MPTF technique.

The paper is organized as follows. The concept of the MPTF technique is outlined in section 2. Section 3 is devoted to the theoretical description of the technique (section 3.2) and the derivation of a minimum phase condition for optical systems (section 3.3). A reader who is mainly interested in the application and results of the technique may however proceed directly to section 4, where the practical requirements of the technique are discussed (section 4.1), and simulated and experimental results are presented for MMICs in SOI without AR coating (sections 4.2 and 4.3). Finally conclusions are drawn.

2. Concept of MPTF

Before describing the MPTF technique, it is convenient to review a basic signal processing concept: the impulse response function [14]. The impulse response function, $m(t)$, of a certain system is the inverse Fourier transform of its frequency response, $M(\nu)$:

$$m(t) = \int_{-\infty}^{+\infty} |M(\nu)| \exp(\mathrm{j}\angle M(\nu)) \exp(\mathrm{j}2\pi\nu t)\mathrm{d}\nu. \tag{1}$$

Here, ν denotes optical frequency, i.e. $\nu = c/\lambda$, with λ the free space wavelength, c the speed of light in vacuum, and $|M(\nu)|$ and $\angle M(\nu)$ are, respectively, the magnitude and phase of $M(\nu)$. In an optical device, $m(t)$ can be thought of as the temporal output that would be recorded when launching an infinitively narrow optical pulse into the system. On the other hand, when measuring an integrated optical system with a TLS and recording the optical output power, the data that is obtained is precisely the power frequency response $|M(\nu)|^2$ (or, equivalently, the power wavelength response $|M(\lambda)|^2$).

To illustrate the concept of MPTF, consider light propagation inside a chip with reflecting facets as shown in Fig. 2(a). C_1 and C_2 are the input and output coupling efficiencies, and R_1, R_2 are the facet amplitude reflectivities. S_{21} and S_{12} represent the device's forward and backward amplitude response, whereas S_{11} and S_{22} are the device's input and output amplitude reflection coefficients. The single mode input and output waveguides are modelled as

$$D_i(\nu) = \exp(-\alpha L_i) \exp(-\mathrm{j}2\pi\nu n_{\mathrm{eff}} L_i/c), \tag{2}$$

with L_i the length of the waveguides, n_{eff} the effective index and α the loss coefficient. For simplicity, here we are neglecting waveguide dispersion. This does not affect our analysis, as long as the temporal effect of a waveguide can be considered to be a delay, i.e. its impulse response is much shorter than the impulse response of the device. The impulse response of

#106382 - $15.00 USD Received 14 Jan 2009; revised 3 Mar 2009; accepted 4 Mar 2009; published 1 May 2009

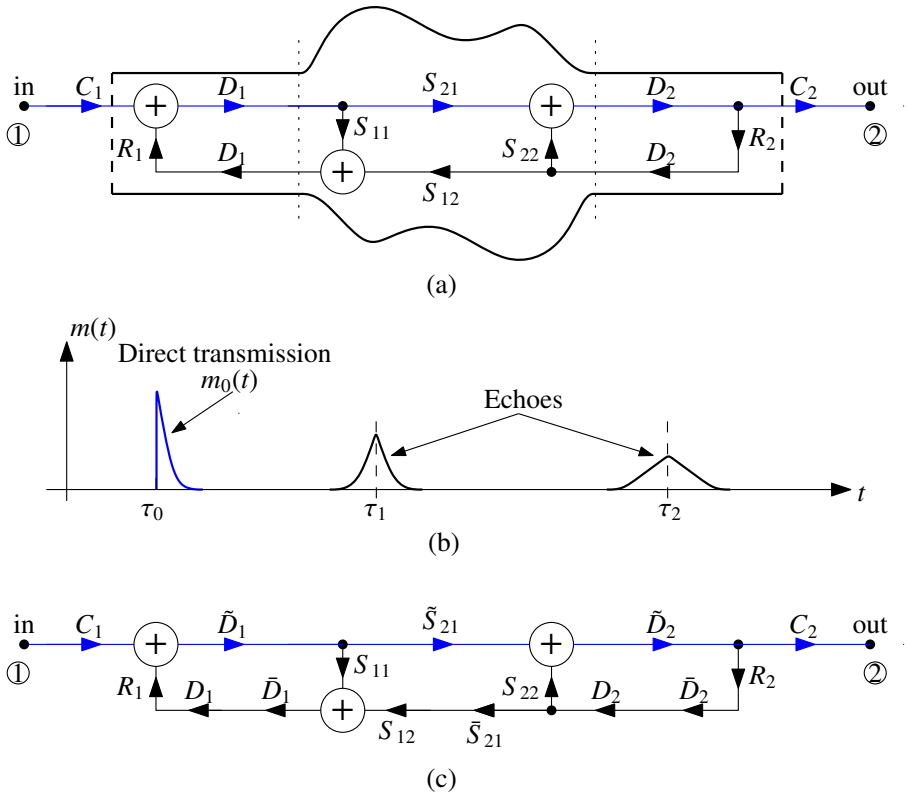

Fig. 2. (a) Physical model of a device inside a Fabry-Perot cavity with signal flow graph. (b) Schematic representation of the impulse response $m(t)$. (c) Minimum phase signal flow graph.

the system in Fig. 2(a) is shown schematically in Fig. 2(b). It will typically consist of a direct transmission term, $m_0(t)$ corresponding to the first transmission through the chip, and a subsequent series echoes arising from internal reflections and facet reflections. The delay of the direct transmission term is τ_0, and the echoes occur at τ_i ($i > 0$).

The MPTF technique recovers the device's forward response, $|S_{21}(\nu)|^2$, from the measured power response of the chip, $|M(\nu)|^2$, using the following steps:

1. Calculate the *minimum* phase response, $\angle\tilde{M}(\nu)$, from $|M(\nu)|$. This is accomplished either by logarithmic Hilbert transformation [15, 14], or using iterative error reduction algorithms [16, 10].

2. Compute the minimum phase impulse response, $\tilde{m}(t)$, as the inverse Fourier transform of $|M(\nu)|\exp(\mathrm{j}\angle\tilde{M}(\nu))$.

3. Filter the unwanted echoes from $\tilde{m}(t)$ and Fourier transform the direct transmission term, $\tilde{m}_0(t)$. As we show in the Section 3.2, the square magnitude of the Fourier transform of $\tilde{m}_0(t)$ yields the direct power transmission through the chip:

$$|\tilde{M}_0(\nu)|^2 = |C_1|^2|C_2|^2\exp(-2\alpha(L_1+L_2))|S_{21}(\nu)|^2. \quad (3)$$

#106382 - $15.00 USD Received 14 Jan 2009; revised 3 Mar 2009; accepted 4 Mar 2009; published 1 May 2009

4. The coupling and waveguide losses are obtained by measuring a reference waveguide and repeating steps 1-3, which yields $|\tilde{W}_0(\nu)|^2 = |C_1|^2|C_2|^2\exp(-2\alpha(L_1+L_2))$. The quotient $|\tilde{M}_0(\nu)|^2/|\tilde{W}_0(\nu)|^2$ then gives the desired parameter $|S_{21}(\nu)|^2$.

Naturally, filtering the direct transmission term is only possible if it is properly separated from the first echo. As discussed in Section 4.1 this is usually the case if the device is not narrow-band, and will be assumed in the following.

3. Theoretical framework

In this section we will provide the theoretical background of the MPTF technique. We proof the applicability of the MPTF algorithm for devices with a single optical path from input to output, as illustrated in Fig. 2(a). In the presence of multiple input and output waveguides, and hence multiple optical paths from input to output, the validity of the technique depends on the minimum phase nature of the device. A sufficient condition for such devices to exhibit minimum phase is derived, assuming, as above, that the separation between echoes be large.

3.1. Laplace transform and minimum phase

Before analyzing the MPTF technique, it is convenient to recall some properties of the Laplace transform. Given a certain impulse response $m(t)$, its Laplace transform,which we will also refer to as transfer function, is defined as

$$M(s) = \int_{-\infty}^{+\infty} m(t)\exp(-st)\mathrm{d}t, \tag{4}$$

where $s = \sigma + \mathrm{j}2\pi\nu$ is the complex Laplace variable. Note that by setting $s = \mathrm{j}2\pi\nu$ in (4) the transfer function reduces to the Fourier transform of $m(t)$, that is, the frequency response $M(\nu)$.

In the following we will use two well known properties of the Laplace transform [14, 11]: i) A transfer function $M(s)$ is a minimum phase function, if and only if, all its poles and zeros are in the left-hand half plane. ii) If $M(s)$ is not minimum phase, it can be factored into a minimum phase function, $\tilde{M}(s)$, and an all pass function, $\bar{M}(s)$. The latter accounts for all the zeros of $M(s)$ in the right-hand half-plane and has unit magnitude, i.e., $|\bar{M}(\nu)| = 1$. From now on the $\tilde{}$ and $\bar{}$ symbols will be used to denote minimum phase and allpass functions, respectively.

3.2. Analysis of MPTF

Consider again the basic device with one input and one output waveguide and reflecting facets shown in Fig. 2(a). We will now analytically examine the application of the MPTF algorithm to this system.

The transfer function of the system in Fig. 2(a) can be obtained using Mason's rule [17], yielding

$$M(s) = \frac{C_1 D_1(s) S_{21}(s) D_2(s) C_2}{\Delta(s)}. \tag{5}$$

The denominator is given by $\Delta = 1 - Q_1 - Q_2 - Q_3 + Q_1Q_2$, the loop gains being $Q_{1,2} = D_{1,2}^2 S_{11,22} R_{1,2}$ and $Q_3 = D_1^2 D_2^2 S_{21} S_{12} R_1 R_2$, where the s dependence has been dropped for simplicity. The numerator is the gain of the only forward path from input to output. In a signal flow graph, a forward path is a path from input to output along which no node is encountered more than once. In an optical device this condition can be understood as the lightwave not travelling through the same waveguide in the same direction more than once. We shall now factor $M(s)$ into a minimum phase function and an all-pass function. Since $M(s)$ is the transfer function of a passive system, it is stable, so that all its poles are in the left-hand half-plane. The zeros of $M(s)$ arise from the zeros of its numerator and the poles of its denominator, $\Delta(s)$. All poles of

#106382 - $15.00 USD Received 14 Jan 2009; revised 3 Mar 2009; accepted 4 Mar 2009; published 1 May 2009

$\Delta(s)$ are in the left-hand half-plane, since all transfer functions involved in the denominator are stable. Hence, the only right-hand half-plane zeros of $M(s)$ are those of its numerator. Thus, $M(s)$ may be factored as $M(s) = \tilde{M}(s)\bar{M}(s)$, with

$$\tilde{M}(s) = \frac{C_1\tilde{D}_1(s)\tilde{S}_{21}(s)\tilde{D}_2(s)C_2}{\Delta(s)} \quad (6)$$

$$\bar{M}(s) = \bar{D}_1(s)\bar{S}_{21}(s)\bar{D}_2(s). \quad (7)$$

The minimum phase and all-pass parts of $D_{1,2}$ are $\tilde{D}_{1,2}(s) = \exp(-\alpha L_{1,2})$ and $\bar{D}_{1,2}(s) = \exp(-sn_{\text{eff}}L_{1,2}/c)$, because $\bar{D}_{1,2}(s)$ has a zero at $\sigma = +\infty$, and $|\bar{D}_{1,2}(s = \text{j}2\pi\nu)| = 1$ (see also [18, Eq. (7)]).

From (6) and (7) we see that $M(s)$ is not a minimum phase function. Consequently, the minimum phase information recovered from the measurement data, $|M(\nu)|^2$, is not the physical phase of the measurement setup, but the phase of a system with transfer function $\tilde{M}(s)$. The signal flow graph of $\tilde{M}(s)$,which is obtained by simple comparison of (5) and (6), is shown in Fig. 2(c). Note that the forward path contains the minimum phase terms, whose product yields the numerator of (6). The all-pass terms have been moved to the lower part of the loops, so that the loops gains (Q_i) that compose the numerator of (6) do not change. From Fig. 2(c) it is clear that the minimum phase impulse response, $\tilde{m}(t)$, is composed of a direct transmission term

$$\tilde{m}_0(t) = C_1C_2\exp(-\alpha(L_1+L_2))\tilde{s}_{21}(t), \quad (8)$$

and a series of echoes from the different feedback loops. If the waveguides are long enough to ensure that the echoes do not overlap with the direct transmission term, which in practical situations is often the case (see Section 4.1), the spurious echoes can be filtered. Fourier transforming the remaining $m_0(t)$ term, and taking the square magnitude of the result we find

$$|\tilde{M}_0(\nu)|^2 = |C_1|^2|C_2|^2\exp(-2\alpha(L_1+L_2))|S_{21}(\nu)|^2, \quad (9)$$

since $|\tilde{S}_{21}(\nu)| = |S_{21}(\nu)|$. This equation is one the main results of this paper. It shows that using the minimum phase information computed from the measurement data, $|M(\nu)|^2$, it is possible to recover the device's magnitude response, $|S_{21}(\nu)|^2$, multiplied by the total waveguide losses, $\exp(-2\alpha(L_1+L_2))$, and the total coupling losses, $|C_1|^2|C_2|^2$. As discussed in Section 2, these losses can be determined by measuring a reference waveguide, so that they can be cancelled from the device measurement. Naturally, this cancellation requires repeatable coupling characteristics, which are achieved if the reference waveguide and the device are close to one another, and their facets are polished to similar quality.

3.3. Minimum phase condition for general device configurations

In the previous section we have shown that in systems with a single forward path the MPTF technique successfully recovers the device response. Let us now consider more complex configurations with multiple forward paths, such as the 2×2 coupler shown in Fig. 3. To determine the minimum phase nature of such a system, it would be possible to explicitly compute the overall transfer function of the device with the reflecting facets and then study the position of its zeros. However, with the signal flow graph approach employed in the previous section, a general minimum phase condition, which provides a better insight into the problem, can be derived. Mason's rule for graphs with N forward paths reads [17]:

$$M(s) = \frac{1}{\Delta(s)}\left[\sum_{k=0}^{N} F_k(s)[1+\sum_{q_k} P_{q_k}(s)]\right], \quad (10)$$

#106382 - $15.00 USD Received 14 Jan 2009; revised 3 Mar 2009; accepted 4 Mar 2009; published 1 May 2009

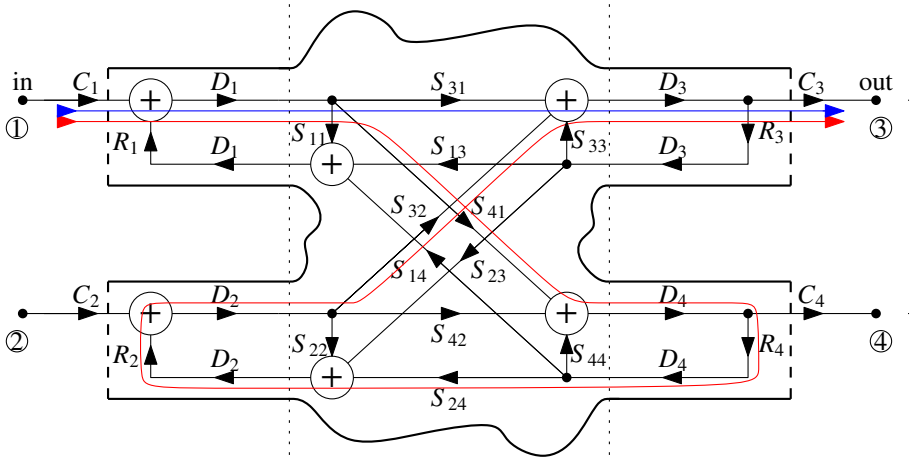

Fig. 3. 2×2 coupler with signal flow graph. The two forward paths are shown as blue and red lines.

where F_k is the gain of the k-th forward path, N is the number of forward paths, and $P_{q_k}(s)$ is a product of loop gains of those loops that do not touch the k-th forward path. Since the numerator of $M(s)$ is now a sum of several terms, $M(s)$ cannot be easily factored into a minimum phase and an all-pass function as in (6) and (7). However, in many practical situation, including multi-mode interference couplers (see Section 4.1), the delay introduced by the waveguides is much larger than the impulse response of the device. As we show in Appendix A, this fact can be exploited to derive a sufficient condition for the minimum phase part of $M(s)$ to contain all the relevant information on the device. This condition is given by

$$|F_0| > \sum_{k=1}^{N} |F_k| + \sum_{k=0}^{N} |F_k| \sum_{q_k} |P_{q_k}|, \tag{11}$$

and is another main result of this paper. It states that *if the gain of the shortest forward path (or direct transmission) is larger then the sum of the gains of the remaining paths (and the relevant loop gains), the associated impulse response is a minimum phase function (with exception of the initial delay).* In the case of a device with a single forward path such as the one analyzed in section 3, (11) holds always, since it reduces to $|F_0| > 0$. This is because if there is only one forward path $N = 0$ and $P_{q_k} = 0$ because all loops touch the forward path.

As an application example of (11) consider the 2×2 coupler illustrated in Fig. 3. Using Mason's rule and dropping the common delay of both forward paths ($D_1 D_3$), we find $V = F_0 + F_1 + F_0 P_0$,where $F_0 = S_{31} C_1 C_3$, $P_0 = R_2 R_4 S_{42} S_{24} D_2^2 D_4^2$ and $F_1 = S_{41} S_{24} S_{32} R_4 R_2 D_2^2 D_4^2 C_1 C_3$. Neglecting waveguide losses and setting $S_{ij} = 1/\sqrt{2}$ $(i \neq j)$, $S_{ii} = 0$, $R_i = 0.56$, which is the approximate Fresnel reflection coefficient for a silicon-air interface as encountered in SOI technology, we find: $|F_0| \approx 0.71 |C_1 C_3| > |F_1| + |F_0||P_0| \approx (0.11 + 0.11)|C_1 C_3|$. Hence, the measured data corresponds to a minimum phase function.

While the derivation of the minimum phase condition (11) is focussed on integrated optical devices, it is expected to hold for more general systems, too, as long as the impulse response consists of short, well separated pulses. In fact, it agrees well with previously published results in other areas. In [10] it was found by simulation that an impulse response with two peaks of comparable magnitude could still be successfully processed using minimum phase techniques, whereas in the presence of a third peak the results were less accurate. Neglecting the P_{q_k} terms

#106382 - $15.00 USD Received 14 Jan 2009; revised 3 Mar 2009; accepted 4 Mar 2009; published 1 May 2009

in (11) and setting $N = 2$, we find $|F_0| > |F_1|$, that is, the impulse response actually remains minimum phase as long as the second peak is only marginally smaller than the first one. On the other hand, for $N = 3$ we have $|F_0| > |F_1| + |F_2|$, which is obviously not fulfilled with three peaks of comparable magnitude, so that the impulse response can no longer be assured to be a minimum phase function. In another paper [21] it is shown experimentally that by artificially adding an impulse at the origin to an arbitrary impulse response function, the sum becomes a minimum phase function. In the treatment presented here this technique consist in increasing the value of $|F_0|$ until (11) holds.

4. Application

The practical application of the MPTF technique is discussed in this section. First, measurement setup requirements are studied and found to be readily realizable. Simulations for MMICs on SOI are carried out and confirm the accuracy of the technique. Finally a 2×3 MMIC on SOI without AR coating is experimentally characterized, and some considerations on the extension of the technique to narrow band devices are given.

4.1. Practical considerations

In this section we will address some practical limitations which have to be taken into account to assure that the algorithm presented in the previous section yields accurate results.

First, and referring to Fig. 2(b), the separation of the first echo and the direct transmission has to be large enough for the two pulses to be clearly separated. The duration of the direct transmission pulse is approximately given by the reciprocal of the couplers bandwidth, whereas the delay of the first echo is bound by the shortest input or output waveguide. From this, the minimum waveguide length is found to be:

$$L_{\min} \gg \frac{\lambda_0^2}{\mathrm{BW}_{\mathrm{DUT}} n_g}, \tag{12}$$

where $\mathrm{BW}_{\mathrm{DUT}}$ is the DUT's 3 dB bandwidth, and n_g is the group index. In micrometer scale SOI rib waveguides the group index is approximately $n_g \approx 3.6$. Assuming a coupler bandwidth $\mathrm{BW}_{\mathrm{DUT}} = 30\,\mathrm{nm}$ at $\lambda_0 = 1550\,\mathrm{nm}$, we find $L_{\min} \gg 20\,\mu\mathrm{m}$, which is verified in virtually any practical layout.

Second, measuring $|M(\nu)|^2$ in a limited bandwidth determines the temporal resolution with which the impulse response can be computed. Equivalently it limits the minimum spatial separation of two reflections that can still be distinguished. Imposing that this separation be the physical length of the device under test, the following criterion for the measurement bandwidth is readily derived:

$$\mathrm{BW}_{\mathrm{meas}} \gg \frac{\lambda_0^2}{L_{\mathrm{DUT}} n_g}. \tag{13}$$

Note that (13) is very similar to the equation that determines the spatial resolution of a OFDR measurements [4, Eq. 8]. For a coupler length of $L_{\mathrm{DUT}} = 300\,\mu\mathrm{m}$, and the same parameters as before, we find $\mathrm{BW}_{\mathrm{meas}} \gg 2\,\mathrm{nm}$. With most moderns lasers sweeping 60 nm or 100 nm of bandwidth is unproblematic, so that condition (13) can be readily fulfilled.

Finally, the required spectral resolution of the measurement is determined by the Nyquist criterion: the sampling of the frequency response has to be fine enough to avoid temporal aliasing of the impulse response, $m(t)$. Taking into account that $m(t)$ consist of a series of echoes from the chip facets, we find:

$$\Lambda \ll \frac{\lambda_0^2}{L_{\max} n_g}, \tag{14}$$

#106382 - $15.00 USD Received 14 Jan 2009; revised 3 Mar 2009; accepted 4 Mar 2009; published 1 May 2009

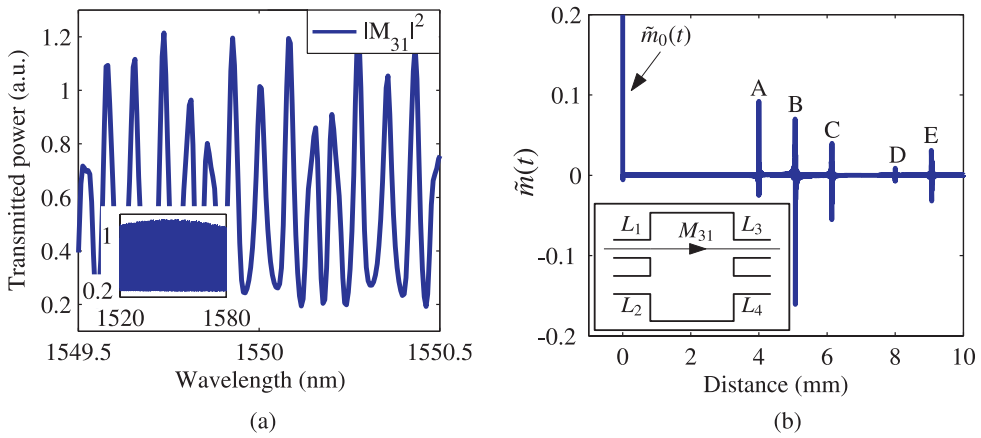

Fig. 4. (a) Simulated power transmission of a 2×2 MMIC in SOI without AR coating. The device layout is shown schematically in the inset of Fig. 4(b). (b) Computed minimum phase impulse response. The length of the input and output waveguides shown in the inset are $L_1 = 1\,\text{mm}$, $L_2 = 2\,\text{mm}$, $L_3 = 3\,\text{mm}$ and $L_4 = 4\,\text{mm}$. The length of the MMIC is 0.256 mm [22].

where Λ is the spectral resolution and $L_{\max}$ is the length of the longest round-trip in the device. A chip length of 1 cm (and an associated round-trip of 2 cm), would require $\Lambda \ll 0.04\,\text{nm}$. The adequate spectral resolution is also easily identified experimentally by ensuring that the interference fringes are smoothly sampled.

4.2. Simulations

We shall now assess the performance of the MPTF technique in two simulated scenarios: a 2×2 and a 2×3 MMIC on SOI with strong reflections from uncoated silicon-air facets.

The transmission and reflection of the couplers and the dispersion characteristics of the input and output waveguides were simulated using the full vectorial eigenmode expansion based Fimmwave software [22]. The reflecting facets were simply modelled as a constant Fresnel reflection amplitude coefficient $R = 0.56$, and perfect coupling was assumed for simplicity. The smoothly varying parameters where then interpolated in Matlab to yield 12000 data points in the 1520 nm to 1580 nm band, i.e., a spectral resolution of 0.005 nm. Using S-parameter network analysis, the reflecting facets, the waveguides and the MMIC were then connected. As expected, the resulting power transmission ($|M_{31}|^2$) through the 2×2 coupler exhibits strong and complex fringes, as shown in Fig. 4(a). The minimum phase of $|M_{31}(\nu)|$ was computed using the logarithmic Hilbert transform approach [15] and the minimum phase impulse response, $\tilde{m}(t)$, was computed through an inverse Fast Fourier Transform (FFT). The processing time for these two operations is about 30 ms using Matlab on a 1.6 GHz notebook. Fig. 4(b) shows $\tilde{m}(t)$, where the time axis has been conveniently scaled to represent propagation distance. Also depicted in Fig. 4(b) are the lengths of the input and output waveguides, which were chosen to illustrate that $\tilde{m}(t)$ has indeed physical meaning. Specifically, the echoes labeled A through E can be associated with different round trips in the coupler. Echo A arises from the propagation through waveguides $1 \to 3 \to 1 \to 3$, which is delayed 4 mm with respect to direct path $1 \to 3$. Echo B results from the trips $1 \to 3 \to 2 \to 3$ and $1 \to 4 \to 1 \to 3$, and C from $1 \to 4 \to 2 \to 3$. D is the echo of the echo of A, and E is a combination of A and B.

A 5 ps wide smooth Kaiser window was used to filter the unwanted echoes and the remaining

#106382 - $15.00 USD Received 14 Jan 2009; revised 3 Mar 2009; accepted 4 Mar 2009; published 1 May 2009

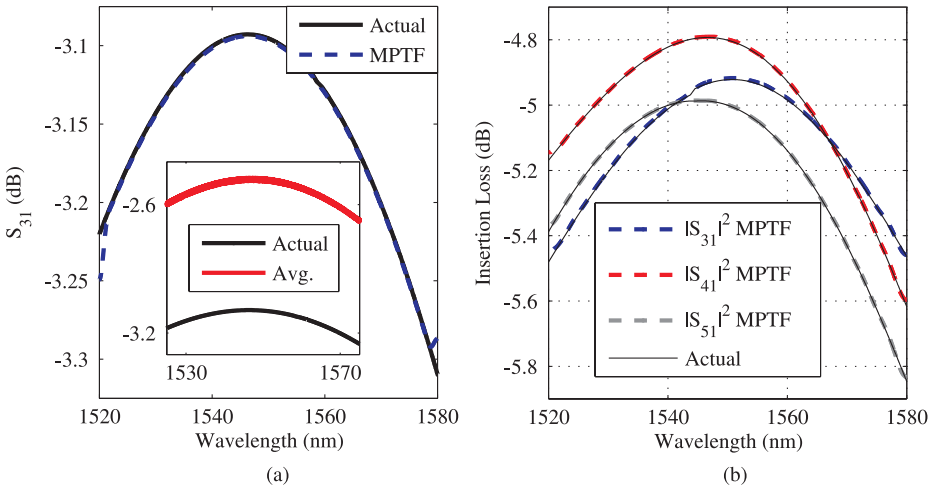

Fig. 5. Recovered coupler parameters for (a) a 2×2 MMIC and (b) a 2×3 MMIC.

direct transmission, $m_0(t)$, was Fourier transformed, yielding the recovered response shown in Fig. 5(a). An excellent agreement between the original response and the MPTF processed data is achieved. The minor deviations at the band edges are an artifact of the Fourier expansion. The inset of Fig. 5(a) demonstrates that simple averaging of the measurement data ($|M_{31}|^2$) does not generally yield accurate results. The 2×3 coupler was simulated with 5.4 mm long input waveguides and 1.9 mm long output waveguides to emulate the physical device layout, and with the same bandwidth and resolution as the 2×2 coupler. The coupler response recovered by MPTF is plotted in Fig. 5(b), and overlaps almost perfectly with the original data, hence confirming the validity of the technique for this coupler configuration, too.

4.3. Experiment

MPTF has been used to experimentally characterize a 2×3 MMIC in SOI without antireflective coating, which was custom fabricated to our specification at the Canadian Photonic Fabrication Center (CPFC). The couplers were etched into a 1.5 μm thick silicon substrate and had a footprint of $12.8 \times 512\,\mu\text{m}^2$. The Fresnel power reflection coefficient at the facets is estimated to be 30%. The measurement setup is depicted in Fig. 6. Linearly polarized light from a tunable laser source (TLS), is converted to horizontally (TE) polarized light using a polarization rotator (PR), and is launched into the chip with a lensed fiber. The output light is collected with a microscope objective, and a polarization beam splitter (PBS) is used to filter unwanted polarization components. Finally, a power detector (PD) converts the optical signal into the electrical domain, where it is recorded with data acquisition board (DAQ). Measurements of the coupler were taken in the 1480 nm to 1580 nm band, with a resolution of 0.001 nm, which takes about one minute using swept measurements. The strong interference patterns in the measurement data are shown in Fig. 1, and are completely masking the coupler response. For calibration purposes a reference waveguide on the same chip as the coupler was also measured. Fig. 7(a) shows the MPTF processed transmission of the reference waveguide, which includes coupling and waveguide losses, as well as laser sweep power nonlinearities. The minimum phase impulse response is plotted in Fig. 7(b), and clearly shows the facet reflection at a distance of ~ 7.7 mm (which corresponds to the length of the chip), as well as a weak back reflection from the MMI

#106382 - $15.00 USD Received 14 Jan 2009; revised 3 Mar 2009; accepted 4 Mar 2009; published 1 May 2009

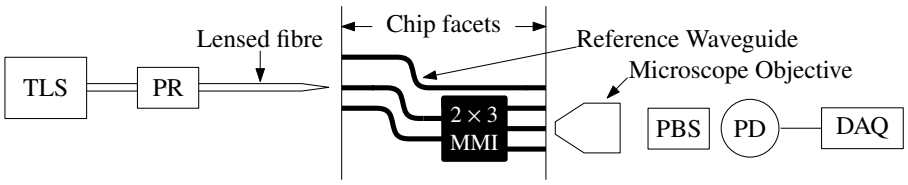

Fig. 6. Measurement setup (not to scale).

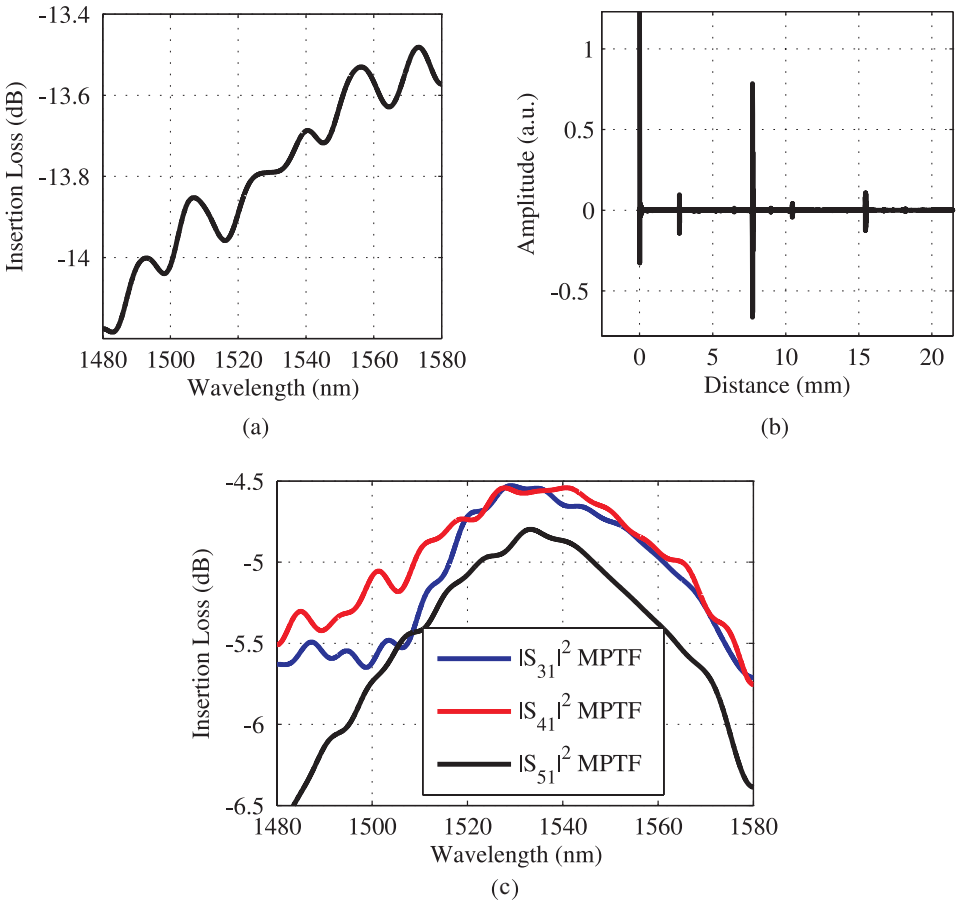

Fig. 7. (a) MPTF processed calibration data. (b) Minimum phase impulse response (c) Recovered coupler response.

at a distance of ~ 2.7 mm. The processed coupler data divided by the reference data is plotted in Fig. 7(c). Due to fabrication tolerances the experimental wavelength response is slightly shifted with respect to the simulated data given in Fig. 5(b), but both the absolute insertion loss as well as the shape of the curves are in good agreement with the simulations.

4.4. Generalization to narrow band devices

While we have focussed our discussion on broadband devices, the MPTF technique could be extended to narrow band devices such as ring resonators. Naturally, these devices must exhibit

#106382 - $15.00 USD Received 14 Jan 2009; revised 3 Mar 2009; accepted 4 Mar 2009; published 1 May 2009

minimum phase, which for ring-resonators is only the case if the coupling coefficient is smaller than the roundtrip losses. To characterize non minimum phase ring resonators, a technique similar to the one described in [21] (see section 3.3) could be used. Since the impulse response of ring resonator is long, the input and output waveguides have to be long enough to avoid overlapping between the direct transmission and the echoes (see Eq. (12)). Finally, the temporal filtering window has to be chosen adequately. If the passband information is of particular importance, smooth temporal windows should be employed. Good reproduction of the resonances requires rectangular windows, which exhibit higher spectral resolution [14, Ch. 11.2].

5. Conclusions

In this paper we have presented the MPTF technique which allows for the accurate characterization of integrated optical devices in the presence of prominent reflections. The technique reconstructs minimum phase time domain information from the measured power transmittance, which is then filtered to eliminate the reflection artifacts. A sufficient condition, Eq. (11), for an optical system to exhibit minimum phase has been established. This condition is in agreement with with previously published experimental results, and can be used to assess the applicability of the MPTF technique. The bandwidth and spectral resolution required to obtain accurate results are readily achievable in practice, and the technique has been successfully applied to 2×2 and 2×3 SOI MMI couplers without antireflective coating in simulation and experiment. These results indicate that the prospects are excellent for implementing this technique as a versatile tool for characterization of integrated waveguide devices.

Appendix A: Derivation of Eq. (11)

Here we derive a sufficient condition for a multi-path device to exhibit minimum phase. The transfer function, $M(s)$, of such a device is given by (10), which is reproduced here for convenience:

$$M(s)=\frac{1}{\Delta(s)}\left[\sum_{k=0}^{N}F_k(s)[1+\sum_{q_k}P_{q_k}(s)]\right].$$

Using the same argument as in section 3.2, it is clear that the denominator of $M(s)$, $\Delta(s)$, does not introduce any non-minimum phase terms, so that we may focus solely on the numerator. Each of the $F_k(s)$ and $P_{q_k}(s)$ terms in (10) is a product of facet reflectivities, R_i, coupling coefficients, C_i, device transmission coefficients $S_{ij}(s)$, and waveguide transmissions $D_i(s)$. If we write the delays of the waveguides explicitly, the numerator of $M(s)$ becomes

$$V(s)=\exp(-s\tau_0)\left[F_0+\sum_{k=1}^{N}F_k\exp(-s\tau_k)+\sum_{k=0}^{N}F_k\exp(-s\tau_k)\sum_{q_k}P_{q_k}\exp(-s\tau_{q_k})\right], \qquad (15)$$

where τ_0 is the delay of the shortest forward path and F_k and P_{q_k} do not depend on the waveguide delays. As discussed in section 3, $\exp(-s\tau_0)$ is an all-pass term, which will be lost when computing the minimum phase response, so we will drop it for the remainder of the discussion. The other delays involved in $V(s)$ must however be conserved when computing the minimum phase response, because they allow for the temporal separation of the direct transmission term from the other forward paths. Consequently, we need to establish a condition that ensures that $V(s)$ be a minimum phase function (with exception of the $\exp(-s\tau_0)$ term).

In many practical situation, including multi-mode interference couplers (see Section 4.1), the delay introduced by the waveguides is much larger than the impulse response of the device. Equivalently, the frequency response of the latter varies very slowly when compared to the former. Hence, for mathematical convenience we may approximate the S_{ij} parameters to be

#106382 - $15.00 USD Received 14 Jan 2009; revised 3 Mar 2009; accepted 4 Mar 2009; published 1 May 2009

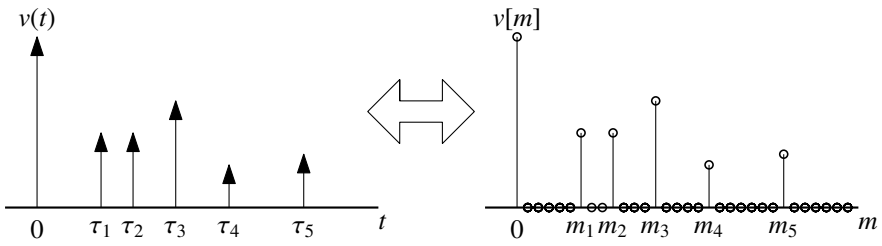

Fig. 8. Discrete time representation of a sequence of impulses.

constants, so that F_k and P_{q_k} in (15) become constants, too. With this simplification $v(t)$, the impulse response function associated with $V(s)$, is simply a finite sequence of impulses with different amplitudes. Consequently, we may treat it as discrete time signal, i.e. as a sampled signal whose amplitude is non-zero only at the position of the impulses (see Fig. 8). The sampled signal can then be z-transformed [19, Ch. 2] yielding $V(z)$, a polynomial in z^{-1}. Let m_M be the degree of this polynomial. For $V(z)$ to be a minimum phase function its zeros must lay inside in the unit circle $|z| = 1$ [19, Ch. 7]. Let us now define $U(z) = z^{m_M} V(z)$ which has the same zeros as $V(z)$ and is given by

$$U(z) = F_0 z^{m_M} + \sum_{k=1}^{N} F_k z^{m_M - m_k} + \sum_{k=0}^{N} F_k z^{m_M - m_k} \sum_{q_k} P_{q_k} z^{-m_{q_k}}. \tag{16}$$

Note that the degree of $U(z)$ is m_M so that it has exactly m_M zeros. We now define the functions

$$f(z) = F_0 z^{m_M} \tag{17}$$

$$g(z) = U(z) - f(z). \tag{18}$$

and invoke Rouché's theorem, which states [20]:

If two functions $f(z)$ and $g(z)$ are analytic inside and on some closed contour γ, and $|f(z)| > |g(z)|$ on γ, then $f(z)$ and $f(z) + g(z)$ have the same number of zeros inside γ.

The functions $f(z)$ and $g(z)$ defined in (17) and (18) are analytic because they are polynomials. Hence, if we impose that $|f(z)| > |g(z)|$ on $|z| = 1$, $U(z) = f(z) + g(z)$ has the same number of zeros inside $|z| = 1$ as $f(z)$. Since $f(z)$ has m_M zeros at $z = 0$, $U(z)$ has m_M zeros inside $|z| = 1$. But $U(z)$ only has m_M zeros in total, so that *all* zeros of $U(z)$ are inside the unit circle. Hence, if $|f(z)| > |g(z)|$ on $|z| = 1$ then $V(z)$ is a minimum phase function. Using the triangle inequality $|z_1 + z_2| < |z_1| + |z_2|$ we thus find that a sufficient condition for $V(z)$ to have all its zeros inside the unit circle is

$$|F_0| > \sum_{k=1}^{N} |F_k| + \sum_{k=0}^{N} |F_k| \sum_{q_k} |P_{q_k}|,$$

which is the expression we were looking for.

Acknowledgments

This work was supported by the Spanish Ministerio de Ciencia e Innovación under project TEC2006-02868, a FPU scholarship with reference number AP-2006-03355, and by the Andalusian Regional Ministry of Science, Innovation and Business (CICYE) under Excellence Research Project TIC-02946. Access to the facilities of the Optoelectronic Devices Group at the National Research Council of Canada is gratefully acknowledged.

#106382 - $15.00 USD Received 14 Jan 2009; revised 3 Mar 2009; accepted 4 Mar 2009; published 1 May 2009